Contrasting oil and gas methane emission intensities across Algeria's major production basins derived using MethaneSAT data

Anthony Himmelberger*[1,^], Mark Omara*[2], Marvin Knapp[2,3], James P. Williams[2], Kaiya Weatherby[2], Ben Lyke[2], Joshua Benmergui[2,3], Katlyn MacKay[2], Jack Warren[2], Luis Guanter[2,4], Steven C. Wofsy[3], Ritesh Gautam[2]

[1] MethaneSAT, LLC, Austin, TX, USA 78701
[2] Environmental Defense Fund, New York, NY, USA 10010
[3] Harvard University, Cambridge, MA, USA 02138
[4] Research Institute of Water and Environmental Engineering (IIAMA), Universitat Politècnica de València, Valencia, Spain

**Correspondence to*: Anthony Himmelberger (anthony.himmelberger@maine.edu), Mark Omara (momara@edf.org)
^Present address: University of Maine, Orono, ME, USA 04401

anthony.himmelberger@maine.edu · momara@edf.org · mknapp@edf.org · jamwilliams@edf.org · kweatherby@edf.org · blyke@edf.org · jbenmergui@methanesat.org · kmackay@edf.org · jwarren@edf.org · lguanter@edf.org · swofsy@seas.harvard.edu · rgautam@edf.org

This is a non-peer-reviewed preprint submitted to EarthArXiv.

Contrasting oil and gas methane emission intensities across Algeria's major production basins derived using MethaneSAT data

Anthony Himmelberger*[1,^], Mark Omara*[2], Marvin Knapp[2,3], James P. Williams[2], Kaiya Weatherby[2], Ben Lyke[2], Joshua Benmergui[2,3], Katlyn MacKay[2], Jack Warren[2], Luis Guanter[2,4], Steven C. Wofsy[3], Ritesh Gautam[2]

[1] MethaneSAT, LLC, Austin, TX, USA 78701
[2] Environmental Defense Fund, New York, NY, USA 10010
[3] Harvard University, Cambridge, MA, USA 02138
[4] Research Institute of Water and Environmental Engineering (IIAMA), Universitat Politècnica de València, Valencia, Spain

Correspondence to: Anthony Himmelberger (anthony.himmelberger@maine.edu), Mark Omara (momara@edf.org)
^Present address: University of Maine, Orono, ME, USA 04401

Abstract. Algeria, Africa's largest natural gas producer and a major European Union gas supplier, has limited basin-scale assessment of oil and gas methane emissions. Here, we use MethaneSAT observations from September 2024 to May 2025 to quantify methane emissions across three Algerian production regions representing 73% of national onshore production. Total methane emissions are 18 t h^{-1} [11–25] in Hassi R'Mel, 25 t h^{-1} [14–39] in Illizi-Ghadames, and 48 t h^{-1} [31–65] in Oued Mya, with gas production-normalized intensities of 0.5%, 1.7%, and 6.9%, respectively. Energy-normalized methane intensities are 0.07, 0.19, and 0.22 kg CH_4 GJ^{-1}, respectively, with oil-dominant Oued Mya exceeding gas-dominant Hassi R'Mel by roughly threefold. Across the three basins, total methane emissions are 85 t h^{-1} [58–113], including ~80 t h^{-1} attributable to oil and gas, at a gas production-normalized intensity of 1.5% and energy-normalized intensity of 0.15 kg CH_4 GJ^{-1}. Our results substantially exceed the 0.2% methane intensity benchmark underpinning the Oil and Gas Decarbonization Charter's near-zero 2030 ambition, and exceed the Global Fuel Exploitation Inventory v3 bottom-up estimate of 61 t h^{-1} by more than 25%. Continued Algerian basin-level monitoring is important for effective methane mitigation, especially as EU Methane Regulation (2024/1787) import intensity thresholds take effect by 2030.

Keywords. satellite remote sensing, atmospheric inversion, top-down emission quantification, bottom-up inventories, methane intensity, gas flaring, EU Methane Regulation

1 Introduction

Methane, as the second most important anthropogenic greenhouse gas after carbon dioxide, is responsible for approximately one-third of current global warming, with a Global Warming Potential more than 80 times that of CO_2 over a 20-year horizon despite its atmospheric lifetime of 12 years (UNEP, 2024; IPCC, 2021). The combination of methane's high radiative forcing and short atmospheric lifetime emphasizes the importance of rapid reductions in methane emissions to limit climate impacts in the near-term (Ocko et al., 2021; EPA, 2023). The fossil fuel sector contributes approximately one-third of global anthropogenic methane emissions, with oil and gas operations contributing through leaks, venting, and incomplete combustion during flaring (IEA, 2024). The

International Energy Agency (IEA) estimates that existing technology can reduce more than 70% of current oil and gas methane emissions, with approximately 30% at no net cost based on 2024 energy prices (IEA, 2025).

The past decade has seen an increased emphasis on methane mitigation through a series of international voluntary commitments spanning government pledges, industry reporting, and operational targets. At the government level, the Global Methane Pledge (launched in 2021; GMP, 2026) committed more than 150 participants to collectively reduce global anthropogenic methane emissions by 30% by 2030 relative to 2020 levels (GMP, 2026). In addition, in 2020, a consortium of oil and gas companies launched the Oil and Gas Methane Partnership 2.0 (OGMP 2.0), which today includes more than 140 member companies committed to reducing oil and gas methane emissions and strengthening emissions measurements at both source- and site-level (UNEP, 2024). The Oil and Gas Decarbonization Charter (OGDC) (launched in December 2023) committed 55 signatory companies representing approximately 35% of combined global oil and gas production to near-zero upstream methane emissions and zero routine flaring by 2030 (OGDC, 2025).

Despite these pledges, global methane concentrations continue to rise (Lan et al., 2025; IEA, 2025), and as of 2024, fewer than 30 Nationally Determined Contributions included “specific measures for reducing energy-related methane emissions, while just 9 included quantitative targets” (IEA, 2025). Some of the world’s largest methane-emitting countries have not joined the GMP, including China, Iran, India, Russia, Venezuela, Syria, Thailand, and Algeria, which account for nearly 45% of global energy-related methane emissions (IEA, 2025). More than 60% of the fossil fuels used in the EU in 2023 were imported (Eurostat, 2025), and the EU Methane Regulation (2024/1787), which began in August 2024, represents the first comprehensive legal framework globally to impose import-related methane emissions requirements on fossil fuels (Regulation (EU) 2024/1787; UNECE, 2025).

Algeria is the largest natural gas producer in Africa and has been a member of the Organization of the Petroleum Exporting Countries (OPEC) since 1969 (EIA, 2025). It is the sixth largest gas-flaring country globally (World Bank GFMR, 2025), and all upstream and export operations are majority-controlled by Sonatrach, the state-owned national oil and gas company (EIA, 2025). Algeria supplied the second-largest share of EU pipeline gas imports in 2024 (Eurostat, 2025) and has consistently been a top-five European gas supplier since 2021 (UK DESNZ, 2025). The importance of Algerian gas imports to the EU has grown since 2022 after the Russian invasion of Ukraine (Tahchi, 2024).

Without any domestic oil and gas methane intensity reporting requirements and until the EU Methane Regulation's import intensity standard takes full effect in 2030, self-reported data in Algeria is currently unreliable and insufficient for regulatory enforcement (Naus et al., 2023). Public oil and gas infrastructure data for Algeria is also limited relative to other major producing countries (Omara et al., 2023), constraining bottom-up inventory development and source attribution. Some previous studies show significant discrepancies between inventories and regional-scale satellite observations in Algeria (Chen et al., 2023; Naus et al., 2023). Naus et al. (2023) used

Sentinel-2 and TROPOMI to study the Hassi R'Mel and Hassi Messaoud oil and gas regions, finding that the UNFCCC-aligned bottom-up inventory overestimated Hassi R'Mel emissions by ~53% and underestimated Hassi Messaoud emissions by ~79%. Chen et al. (2023) similarly found that oil and gas emissions across the Middle East and North Africa are driven more by infrastructure and management practices than by production volumes. However, neither study provides individual basin-scale comparison across multiple regions with contrasting production types, leaving important gaps in understanding how oil and gas production characteristics may drive emissions and emissions intensity variability across Algeria.

MethaneSAT, which launched in March 2024 and operated until June 2025, was designed to monitor oil and gas methane emissions from space and bridge a critical observational gap between coarse-resolution global mappers such as TROPOMI and GOSAT and narrow-swath point-source detection imagers. With a wide swath of ~220 km and spatial resolution of 110 m × 400 m at nadir, MethaneSAT measured the atmospheric column-averaged dry-air mixing ratio of methane with a precision of 25–55 ppb at native pixel scale, enabling high-resolution, spatially resolved quantification of dispersed area emissions across oil and gas basins (MethaneSAT, 2025; Jacob et al., 2022; Guanter et al., 2026; Williams et al., 2026). Over its 13-month operational lifetime (May 2024–June 2025), MethaneSAT collected data over oil and gas production regions that account for ~50% of global onshore oil and gas production, providing the basis for a global assessment of regional methane emissions and intensities across major producing basins.

Here, we quantify methane emissions across three of Algeria's major production basins, Hassi R'Mel, Oued Mya, and Illizi-Ghadames, using MethaneSAT observations between September 2024 and May 2025. These basins represent three types of production: gas-dominant, oil-dominant, and mixed-production, respectively, providing insight into how methane intensities vary across diverse oil and gas production profiles. We evaluate trends in oil and gas production and gas flaring, compare with other satellite-based measurements and "bottom-up" inventories, and discuss methane emissions intensity relevance for the EU's emerging import compliance framework.

2 Study areas and methods

2.1 Three study regions

North Africa is rich in oil and gas reserves, with over 220 petroleum discoveries across the countries of Libya, Tunisia, and Algeria (Albriki et al., 2022). In this research, we examine 19 MethaneSAT observations in Algeria, 7 in the Hassi R'Mel, 8 in the Oued Mya, and 4 in the Illizi-Ghadames basin (Fig. 1). Each region is named after the primary oil and gas basin or field it encompasses and together represent the full spectrum of Algeria's hydrocarbon production, from one of Africa's largest dry gas fields to mature oil-dominant fields, providing a unique opportunity to assess how production type correlates with methane emissions.

The Hassi R’Mel, first discovered in 1956, is Algeria’s largest natural gas field and one of the largest in the world with proved reserves of 85 trillion cubic feet (Tcf), estimated to hold more than half of Algeria’s total gas reserves (EIA, 2025), a gas share of 87%, and 2024 total oil and gas production of 912 kboe d^{-1} (EIA, 2025; Wood Mackenzie, 2024). It serves as a hub connecting to the Trans-Mediterranean pipeline in Italy, the Medgaz pipeline in Spain, and LNG terminals at Arzew and Skikda (EIA, 2025).

The Oued Mya basin, also first discovered in 1956, is home to Algeria's largest oil field, Hassi Messaoud, with a gas share of 17% and 2024 total oil and gas production of 842 kboe d^{-1}. The Hassi Messaoud complex comprises four fields that are majority-operated by Sonatrach (Global Energy Monitor, 2025a; Wood Mackenzie, 2024).

The Illizi-Ghadames, first discovered in 1957, is a mixed-production basin with some of North Africa's most prolific petroleum provinces, a gas share of 61%, and 2024 total oil and gas production of 558 kboe d^{-1}. It has the second most oil reserves in the country and connects to the Hassi R’Mel region via the major Alrar-Hassi R’Mel pipeline (Galeazzi et al., 2010; Global Energy Monitor, 2025b; Wood Mackenzie, 2024).

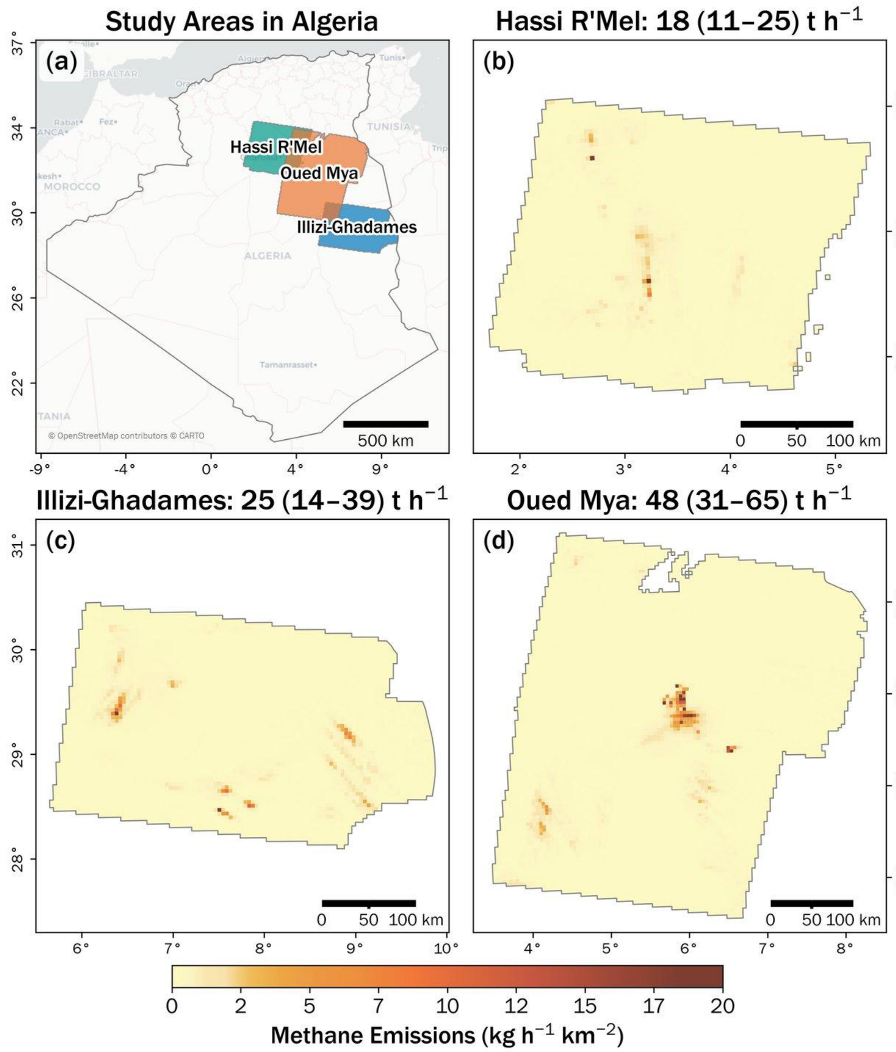

Figure 1. (a) Location of the three study regions within Algeria. (b–d) Spatially explicit mean total methane area emissions (kg h^{-1} km^{-2}) from MethaneSAT observations across three oil and gas production regions: (b) Hassi R'Mel, (c) Illizi-Ghadames, and (d) Oued Mya. Values in panel titles indicate mean total area methane emissions in t h^{-1} with 95% confidence intervals, averaged across 7, 4, and 8 MethaneSAT collections, respectively, spanning September 2024–May 2025.

2.2 Methods

We produce methane emission maps for 19 MethaneSAT collections (Table 1) using the Column Observations to Regional Emissions (CORE) inversion framework. A detailed description of the CORE Level-4 emissions inversion process is provided in the MethaneSAT L4 Algorithm Theoretical Basis Document (MethaneSAT Science and Engineering Team, 2026). CORE relates observed column-averaged mole fractions (XCH_4) to surface fluxes using source-receptor relationships computed via the Stochastic Time-Inverted Lagrangian Transport (STILT) model (Lin et al., 2003; Fasoli et al., 2018). Prior emission rates are derived from global, annual mean emissions reported by East et al. (2025) at 25 km resolution. The prior preserves the East et al. (2025) emissions in most areas but imposes a minimum emission rate of 1 kg h^{-1} km^{-2}, enabling CORE to identify emissions anywhere. We assign a prior uncertainty based on the expected temporal variability of the sector that dominates the local emissions; e.g., we assign a high variability to the emission from the oil and gas sector and a lower variability to the livestock sector. CORE uses MethaneSAT data to compute expectation values of surface fluxes at 4 km resolution employing Monte Carlo sampling (Carpenter et al., 2017; Hoffman and Gelman, 2011). Reported surface fluxes represent emission estimates over the scene-specific ventilation period, reaching up to 28 hours prior to observation. We report composite scenes in these three basins following the methods described in Williams et al. (2026). First, we construct a shared grid from the union of the observed collection footprints, pooling the vectorized per-collect emission pixels, preserving mass without reprojection. Next, each grid cell's average value is calculated per pixel, creating an aggregated output that equally weights each collection.

Uncertainty in aggregated emissions is propagated using a Monte Carlo approach, drawing from each grid cell's MCMC posterior distribution (n = 4,000) and applying an additional 20% term representing atmospheric transport error, with 95% confidence intervals derived from the 2.5th and 97.5th percentiles of the resulting aggregate distribution (Williams et al., 2026).

We allocate total aggregated methane emissions from MethaneSAT to the oil and gas sector using a literature-based subtraction of an estimated representative mean non-oil and gas contribution from the total emissions. To do this, we compile literature-based estimates of non-oil and gas emissions from both top-down and bottom-up sources that report sectorally disaggregated emissions (Worden et al., 2022; East et al., 2025; Crippa et al., 2024; Granier et al., 2019). We use the mean of these non-oil and gas estimates and subtract it from the total methane emissions for each basin to produce an estimate of oil and gas methane emissions. This method is similar to the approach used in MacKay et al. (2026) for MethaneAIR measurements in the US (see also Alvarez et al., 2018). We also test a composite prior-based methodology like in Williams et al. (2026) but find that it produces higher proportions of non-oil and gas emissions than would be expected in barren desert regions of the Hassi R'Mel, based on prior literature (East et al. 2025). We further discuss this testing in the Supplement (Sect. S1).

We use field-level oil and gas production data from Wood Mackenzie (2020–2024) and gas flaring data from the VIIRS satellite for 2020–2024 (World Bank GFMR, 2024) to calculate gas share and production and flaring trends. Total production reported in kboe d^{-1} (thousand barrels of oil equivalent per day) uses a standard conversion of 1 BOE = 6 Mcf for gas and 1 BOE = 5.71 GJ for energy intensity calculations. The oil and gas sectoral output is used to calculate marketed gas production-normalized methane intensity (also referred to as loss rate; emissions / (marketed gas production × methane composition); Alvarez et al., 2018) and energy-normalized methane intensity (oil and gas emissions divided by total energy production, in kg CH_4 GJ^{-1}), using an area-adjusted production calculation for Wood Mackenzie production fields spanning domain boundaries. We use a uniform methane composition of 0.90 for all three regions, as we normalize emissions by marketed gas production, expected to be of pipeline-quality gas specifications, similar to the approach in recent studies (Alvarez et al., 2018; Shen et al., 2023). We test the sensitivity of marketed gas production-normalized intensity calculations to this assumption in the

Supplement (Sect. S2). Energy-normalized intensity does not incorporate a methane composition assumption and is therefore directly comparable across studies.

Table 1. Summary of MethaneSAT collections used in this study across three oil and gas production basins in Algeria. Observation dates span September 2024–May 2025. Total methane emissions and full observation domain emissions are reported with 95% confidence intervals. Area covered refers to the spatial extent of valid retrievals within each collection.

Region	Observation date	Area covered (km^2)	Total methane emissions ($t\ h^{-1}$) [95% c.i.]	Full observation domain ($t\ h^{-1}$) [95% c.i]
Hassi R'Mel	9 September 2024	22,010	4 [1–10]	18 [11–25]
	23 September 2024	36,530	14 [8–22]	
	24 September 2024	37,550	14 [7–25]	
	5 October 2024	38,130	13 [7–22]	
	5 November 2024	53,070	11 [7–18]	
	18 November 2024	42,065	10 [4–20]	
	21 December 2024	49,120	15 [8–25]	
Illizi-Ghadames	17 November 2024	56,030	11 [5–18]	25 [14–39]
	30 December 2024	21,920	11 [3–24]	
	17 January 2025	60,400	17 [10–27]	
	17 May 2025	35,120	14 [7–23]	
Oued Mya	11 September 2024	82,160	21 [13–33]	48 [31–65]
	15 November 2024	28,400	5 [2–11]	
	17 November 2024	21,970	27 [19–37]	
	19 December 2024	51,460	9 [4–16]	
	18 January 2025	69,530	16 [8–27]	
	20 January 2025	49,520	13 [7–22]	
	22 February 2025	32,390	11 [4–22]	
	31 March 2025	62,840	35 [21–53]	

MethaneSAT observations enable direct comparison with both previous satellite inversions (top-down) and emission-factor-based emissions inventories (bottom-up), helping contextualize the accuracy and utility of bottom-up inventories. We compare our aggregated total methane emissions outputs to other spatially explicit methane emissions datasets through spatial domain clipping. Our analysis utilizes the bottom-up inventories of EDGARv8.0

(version EDGAR_2025_GHG; Crippa et al., 2024) and CAMS v6.2 (Granier et al., 2019), both for 2024, as well as GFEI v3 (Scarpelli et al., 2025) for the year 2020. We also use several top-down studies, including East et al. (2025) (TROPOMI and GHGSAT for 2023), Shen et al. (2023) (TROPOMI for 2018–2020), Worden et al. (2022) (GOSAT for 2019) and Chen et al. (2023) (TROPOMI for 2019). We further compare our outputs by clipping MethaneSAT emissions to the georeferenced Naus et al. (2023) domain boundaries for the Hassi R'Mel and Hassi Messaoud regions (Fig. 5). A country-wide comparison with IEA (2024) estimates and an IEA emissions factor analysis are presented in the Supplement (Sects. S3–S4).

3 Results and Discussion

3.1 MethaneSAT analysis of methane emissions and intensity

We aggregate 19 MethaneSAT collections from September 2024 through May 2025 (see Table 1). Total methane emissions are 18 [11–25] t h^{-1} in the Hassi R'Mel, 48 [31–65] t h^{-1} in the Oued Mya, and 25 [14–39] t h^{-1} in the Illizi-Ghadames (Fig. 2, left). Marketed gas production-normalized methane intensities also vary by basin, with 0.5% [0.2–0.7%] in Hassi R'Mel, 1.7% [0.9–2.7%] in Illizi-Ghadames, and 6.9% [4.1–10.1%] in Oued Mya. Marketed gas production-normalized methane intensity decreases with increasing gas share across the three basins. Despite comparable total oil and gas production (842 vs. 912 kboe d^{-1}), the 83% oil-dominant Oued Mya shows total methane emissions more than 2.5 times higher than the 87% gas-dominant Hassi R'Mel (48 t h^{-1} [31–65] vs. 18 t h^{-1} [11–25]) and a marketed gas production-normalized methane intensity more than 13 times higher (6.9% vs. 0.5%). Energy-normalized methane intensities, which account for total energy (oil and gas) production rather than gas alone, show a narrower range: 0.07 [0.04–0.11] kg CH_4 GJ^{-1} in Hassi R'Mel, 0.19 [0.097–0.30] kg CH_4 GJ^{-1} in Illizi-Ghadames, and 0.22 [0.13–0.32] kg CH_4 GJ^{-1} in Oued Mya. Combined across the three regions, total methane emissions are ~85 t h^{-1} [58–113], with ~80 t h^{-1} attributable to oil and gas, at a combined marketed gas production-normalized methane intensity of 1.5% [0.94–2.1%] and energy-normalized intensity of 0.15 [0.094–0.21] kg CH_4 GJ^{-1}.

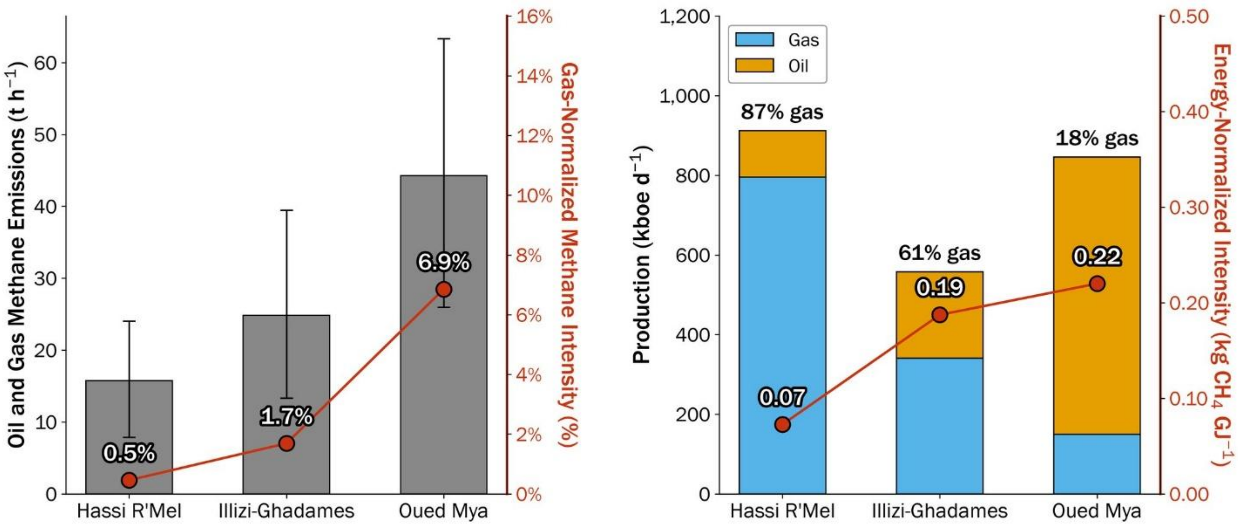

Figure 2. Summary of oil and gas methane emissions and production across the three study regions. (Left) oil and gas methane emissions (t h^{-1}) with 95% confidence intervals (error bars), gas-normalized methane intensity (%, red dots). (Right) Total oil and gas production (kboe d^{-1}) with energy-normalized methane intensity (kg CH_4 GJ^{-1}, red dots) and gas share. Mean marketed gas production-normalized intensity shows a more than 13-fold range (0.5–6.9%), while energy-normalized intensity's range is narrower (0.07–0.22 kg CH_4 GJ^{-1}).

Gas flaring varies year-to-year across all three regions from 2020–2024. Illizi-Ghadames shows a sustained decline (-31%), while Hassi R'Mel and Oued Mya fluctuate around their 2020 levels, with 2024 endpoint values lower (-13% and -14%, respectively) but no clear downward trend. Oil and gas production in the Hassi R'Mel is stable, with a 1% increase from 2020–2024, while production in the Illizi-Ghadames has decreased 8% and production in the Oued Mya has increased 10% (Fig. 3).

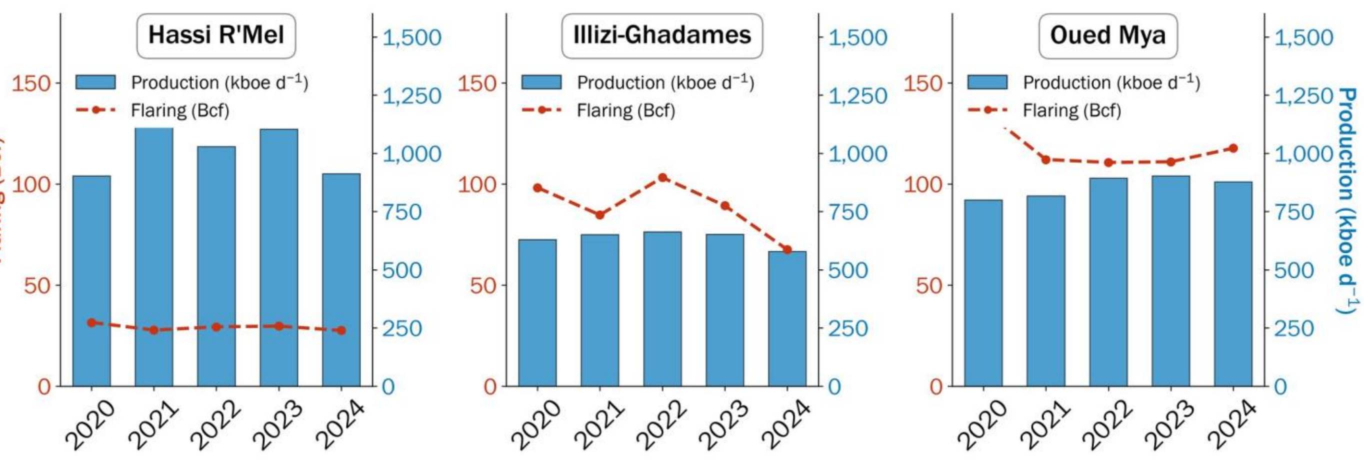

Figure 3. VIIRS-based gas flaring volumes (Bcf) (orange lines, left axis) and Wood Mackenzie total marketed oil and gas production (blue bars, right axis) for the Hassi R'Mel (left panel), Illizi-Ghadames (middle panel), and Oued Mya (right panel) regions from 2020–2024. Illizi-Ghadames shows a sustained flaring decline (-31%), while Hassi R'Mel and Oued Mya fluctuate around 2020 levels (-13% and -14% at 2024 endpoint, respectively, but no clear downward trend). Oil and gas production remains stable or increases across all three basins.

3.2 Comparison with previous methane emission estimates

We compare our total methane emissions for the three regions with other top-down and bottom-up studies (Fig. 4), while acknowledging the differences in the year of measurements or estimates across studies. In the Hassi R'Mel, three older satellite-based estimates (Chen et al., 2023; Shen et al., 2023; Worden et al., 2022) range from 66 to 111 t h^{-1}, roughly four to six times MethaneSAT's 18 t h^{-1} [11–25], while the more recent East et al. (2025) TROPOMI/GHGSat estimate of 9 t h^{-1} is the closest published value to ours, at roughly half our estimate. This overall overestimation from older top-down measurements is consistent with Naus et al. (2023) finding that the UNFCCC-aligned bottom-up inventory overestimated Hassi R'Mel emissions by ~53%. In the Illizi-Ghadames basin, MethaneSAT's total of 25 t h^{-1} [14–39] sits within the range of previous top-down measurements (25–51 t h^{-1}). Oued Mya MethaneSAT totals (48 t h^{-1} [31–65]) sit within the range of top-down inversions (37–78 t h^{-1}), in the middle of the published range. For bottom-up comparisons, Hassi R'Mel's 18 t h^{-1} [11–25] is below the range of bottom-up inventories (19–41 t h^{-1}), Illizi-Ghadames total of 25 t h^{-1} [14–39] is within the bottom-up range (21–71 t h^{-1}), and Oued Mya total of 48 t h^{-1} [31–65] falls within the range of bottom-up inventories (17–76 t h^{-1}), comparable to EDGAR (53 t h^{-1}). MethaneSAT aggregated totals sit at or below the lower end of nearly all prior published estimates, with the largest gap in the gas-dominant Hassi R'Mel.

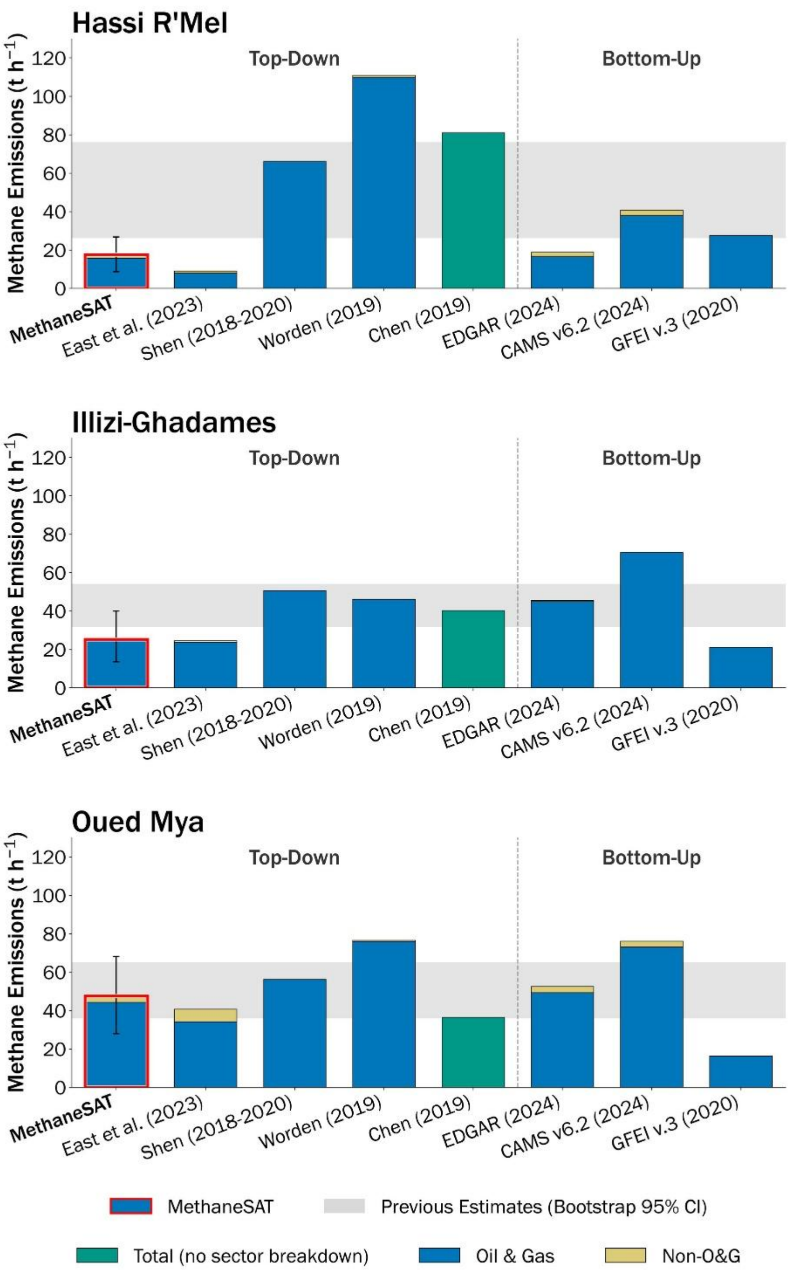

Figure 4. Comparison of MethaneSAT aggregated total methane emissions with previous top-down satellite inversions and bottom-up inventories for each basin. The MethaneSAT bar (outlined in red, with 95% confidence intervals) is disaggregated into oil and gas (blue) and non-oil and gas (yellow) sectoral components. Previous estimates are shown disaggregated into oil and gas and non-oil and gas components where available; Chen et al. (2023) reports a total only. Note that previous estimates span different instruments, methodologies, and spatial resolutions; study time periods are shown in parentheses.

We also compare total methane emissions with Naus et al. (2023), who used Sentinel-2 and TROPOMI to estimate total atmospheric methane in the Hassi R'Mel and Hassi Messaoud (within the Oued Mya basin) regions for 2020 (see Fig. 5). We match the spatial domains between Naus et al. (2023) and MethaneSAT to ensure accurate comparison. Naus et al. (2023) estimated 18.3 t h^{-1} [12.6–25.1] in the Hassi R'Mel and 25.1 t h^{-1} [14.8–32.0] in the Hassi Messaoud, compared to 16 t h^{-1} [9–25] in the Hassi R'Mel and 29 t h^{-1} [17–41] in the Hassi Messaoud from

MethaneSAT (Table 2). The MethaneSAT-Naus intersection captures 100% of gas production in the Hassi R'Mel but only ~71% in the Oued Mya.

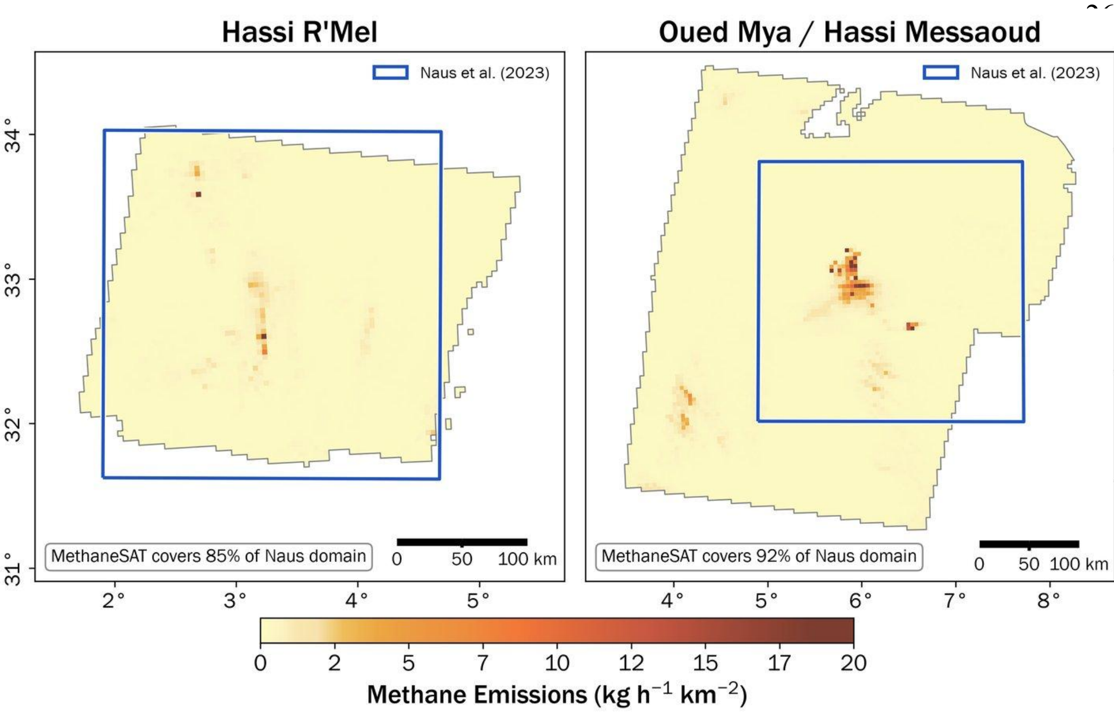

Figure 5. Mean total methane area emissions (kg h^{-1} km^{-2}) from MethaneSAT observations in the Hassi R'Mel (left) and Oued Mya / Hassi Messaoud (right) regions, with Naus et al. (2023) domain boundaries shown in blue. MethaneSAT spatial coverage extends beyond the Naus domains in both regions, covering 85% of the Naus domain area in the Hassi R'Mel and 92% in the Oued Mya / Hassi Messaoud. The MethaneSAT-Naus intersection captures 100% of gas production in the Hassi R'Mel and 71% in the Oued Mya.

Table 2. Comparison of total methane emissions with Naus et al. (2023) for the Hassi R'Mel and Hassi Messaoud / Oued Mya regions. Naus et al. (2023) estimates are derived from Sentinel-2 and TROPOMI for 2020; this study reports MethaneSAT total emissions clipped to the Naus et al. (2023) domain boundaries for 2024/2025. Both studies report total methane emissions rather than sectorally-attributed oil and gas methane emissions. Confidence intervals for this study are derived by applying the fractional uncertainty from the full MethaneSAT domain to the clipped emission totals, assuming spatially uniform relative uncertainty across the domain. Domain boundaries do not perfectly overlap (see Fig. 5).

	Naus et al. (2023) 2020	This study 2024/25
Hassi R'Mel emissions	18.3 [12.6–25.1] t h^{-1}	16 [9–25] t h^{-1}
Hassi Messaoud / Oued Mya emissions	25.1 [14.8–32.0] t h^{-1}	29 [17–41] t h^{-1}

Overall, this study provides a detailed basin-scale, high-resolution comparison across three of Algeria's major oil and gas production basins. We find a large range in marketed gas production-normalized methane intensity, from 0.5% in the Hassi R'Mel to 6.9% in the Oued Mya, consistent with production type as the primary driver, with the 87% gas-dominant Hassi R'Mel demonstrating low intensity in comparison to the 83% oil-dominant Oued Mya (only 17% of the total energy is from gas). Energy-normalized methane intensities, which account for total oil and gas production rather than gas alone, show a narrower range (0.07 kg CH_4 GJ^{-1} in Hassi R'Mel to 0.22 kg CH_4 GJ^{-1} in Oued Mya), compared to the more than 13-fold marketed gas production-normalized range. We advance upon the prior work of Naus et al. (2023) and Chen et al. (2023) with MethaneSAT, which provides higher spatial resolution and adds the Illizi-Ghadames basin to the comparison, a mixed-production basin.

To contextualize Algeria's methane intensities against well-characterized producing regions in the United States, we compare each region to a structurally similar U.S. basin measured by MethaneAIR (MacKay et al., 2026) and MethaneSAT (Williams et al., 2026), primarily considering similarities in basin-level oil and gas production profiles. We rescale U.S. marketed gas production-normalized intensities to a common methane composition of 0.90 for direct comparison (see Sect. S5, Table S4). The gas-dominant Hassi R'Mel (87% gas) outperforms the Haynesville-Bossier basin (99% gas; MacKay et al., 2026) on both metrics: adjusted marketed gas production-normalized methane intensity (0.5% vs. 0.9%; MacKay et al., 2026) and energy-normalized methane intensity (0.07 vs. 0.15 kg CH_4 GJ^{-1}; MacKay et al., 2026), suggesting Hassi R'Mel performs at or above the level of well-operated gas-dominant U.S. basins. The mixed-production Illizi-Ghadames (61% gas) shows marketed gas production-normalized methane intensity comparable to the Eagle Ford basin (1.7% vs. 1.6–2.1%; MacKay et al., 2026; Williams et al., 2026), with similar agreement on energy-normalized methane intensity (0.19 vs. 0.13–0.21 kg CH_4 GJ^{-1}). The oil-dominant Oued Mya (83% oil) is approximately three times higher than the Permian basin (~60% oil dominant; MacKay et al., 2026; Williams et al., 2026) on marketed gas production-normalized methane intensity (6.9% vs. 2.1–2.3%) and roughly 40% higher on energy-normalized methane intensity (0.22 vs. 0.15–0.16 kg CH_4 GJ^{-1}), indicating that Oued Mya's underperformance persists even after accounting for its oil-dominant production mix. Our comparisons of energy-normalized methane intensities are not subject to the methane composition caveat and are directly comparable across studies. The strong performance of Hassi R'Mel relative to Haynesville-Bossier suggests that dry gas infrastructure operating under similar design objectives can match or exceed the emissions performance of U.S. analogs. The underperformance of Oued Mya relative to its U.S. analog, particularly on energy-normalized intensity, likely reflects differences in gas capture infrastructure and operational practices in oil-dominant production settings.

Higher spatial resolution satellite observations and inversions capture emissions that coarser inversions may miss or overestimate, depending on oil and gas production type, though differences in study period, inversion methodology, and the use of prior ('bottom-up') emissions data in the inversions also contribute to disagreements across estimates. In the gas-dominant Hassi R'Mel, previous top-down estimates are roughly four to six times higher than MethaneSAT (66–111 t h^{-1} vs. 18 t h^{-1} [11–25]) (Chen et al., 2023; Shen et al., 2023; Worden et al., 2022) (see Fig. 4). Naus et al. (2023) similarly found bottom-up inventories aligned with UNFCCC reports overestimated Hassi R'Mel emissions by ~53% (24–73%), while other studies suggest that coarser resolution may smear emissions from surrounding sources into gas-dominated regions (Tibrewal et al., 2024; Jacob et al., 2022). In the oil-dominant production basin of Oued Mya, MethaneSAT totals (48 t h^{-1} [31–65]) sit within the range of top-down inversions (37–78 t h^{-1}) and within the range of bottom-up inventories (GFEI v3: 17 t h^{-1}; EDGAR: 53 t h^{-1}; CAMS: 76 t h^{-1}), comparable to EDGAR at the middle of the bottom-up range. MethaneSAT's higher spatial resolution of emissions products (~4 km × 4 km vs. 25 km × 30 km to 200 km × 250 km TROPOMI vs. ~100 km × 100 km to 400 km × 500 km GOSAT) likely contributes to the closer agreement with bottom-up inventories than with older top-down inversions, though differences in study period and inversion priors may also contribute to these discrepancies. Chen et al. (2023) similarly found that oil and gas methane emissions across the Middle East and North Africa are driven more by infrastructure and management practices than by production volumes, consistent with the contrasting patterns we observe between Hassi R'Mel and Oued Mya. The wide disagreements from previous estimates underscore the value of MethaneSAT's higher spatial resolution (Jacob et al., 2022), while also highlighting the difficulty of attributing discrepancies to any single methodological factor.

Naus et al. (2023) used Sentinel-2 and TROPOMI to estimate total methane emissions in the Hassi R'Mel and Hassi Messaoud (within the Oued Mya basin) regions for 2020 (Table 2). The domains used in Naus et al. (2023) do not perfectly match ours (see Fig. 5), and our clipped totals are 10% lower in the Hassi R'Mel (16 t h^{-1} vs. 18 t h^{-1}) and 16% higher in the Hassi Messaoud (29 t h^{-1} vs. 25.1 t h^{-1}). These differences are not statistically significant (Hassi R'Mel: $p = 0.76$; Hassi Messaoud: $p = 0.67$), likely reflecting the combination of different study periods (2020 vs. 2024/2025), instrument characteristics, and incomplete domain overlap rather than a systematic emissions change. Note that the MethaneSAT-Naus intersection captures only ~71% of gas production in the Oued Mya and that Naus et al. (2023) reports total methane emissions from all sources rather than oil and gas sectoral emissions, precluding direct comparison of oil and gas methane intensities.

3.3 Limitations

This study utilizes 19 MethaneSAT collections from September 2024 to May 2025 with no summer collections, which means no coverage for any possible temperature-associated fugitives or maintenance cycle changes. Our data aggregation is able to account for emissions persistence to a degree; however, these collections each represent a quasi-daily emissions estimate of up to 28 hours, and individual scenes can vary substantially due to partial domain coverage, episodic emissions, and transport variability (Table 1). Illizi-Ghadames, with 4 collections, is subject to larger uncertainties than Hassi R'Mel and Oued Mya, although MethaneSAT's high-precision measurements are designed to quantify regional emissions even from individual observations (Jacob et al., 2022). This study uses a uniform methane composition of 0.90 for all three regions, based on pipeline-quality marketed gas specification assumptions (Alvarez et al., 2018; Shen et al., 2023). Actual gas composition for gas sent to sales varies by field within each region, which introduces uncertainty in methane intensity calculations. Additionally, production data relies on Wood Mackenzie field-level estimates with area-adjusted allocation for fields spanning domain boundaries, which may not reflect actual well-level production distribution. The three regions in this study represent 73% of Algeria's total onshore production, so results may not generalize to unobserved areas, particularly to regions with different production profiles.

3.4 Policy implications

Algeria is a non-Annex I party under the UNFCCC, meaning it submits National Communications and Biennial Update Reports. The GFEI v3 inventory (Scarpelli et al. 2025) spatially disaggregates national emissions reported to the UNFCCC, making it the closest proxy of Algeria's officially reported oil and gas emissions, and we find our three-region MethaneSAT oil and gas methane emissions of ~80 t h^{-1} to exceed GFEI's 2020 estimate for the same three-basin domain (61 t h^{-1}; Scarpelli et al., 2025) by more than 25%. Although the three-basin aggregate methane emissions intensity is 1.5%, this obscures the vast difference between the Hassi R'Mel (0.5%) and Oued Mya (6.9%) and highlights the importance of basin or region-level differentiation when tracking methane intensity thresholds. However, the choice of intensity metric significantly affects this comparison: energy-normalized methane intensity, which accounts for total oil and gas production rather than only gas, narrows the range from more than 13-fold to roughly threefold (0.07 vs. 0.22 kg CH_4 GJ^{-1}). For oil-dominant basins like the Oued Mya, where gas capture may not be the foremost priority, energy-normalized intensity is the more appropriate metric (Seymour et al. 2025). Algeria, as the second-largest gas supplier of EU pipeline gas in 2024 after Norway (Eurostat, 2025), will be subject to EU Methane Regulation (2024/1787) import intensity thresholds expected to take effect by 2030 (Talus et al., 2024). The satellite-derived methane emissions intensity is significantly larger than the 0.2% of marketed gas production that the Oil and Gas Climate Initiative (OGCI) set as its collective methane intensity ambition, which underpins the Oil and Gas Decarbonization Charter's goal of near-zero upstream methane emissions by 2030 (OGCI, 2024; OGDC, 2025).

Algeria's absence from these frameworks is unsurprising given that there are no domestic methane reporting requirements under Law 19-13 (IEA, 2022). The IEA estimates that more than 70% of current oil and gas methane emissions can be prevented, and ~30% of those can be mitigated at no net cost (IEA, 2025), yet Algeria has not been positioned to leverage this potential. With 47% of government revenue and 84% of export revenue coming from oil and gas (IMF, 2024), there appears to be a substantial emissions reduction opportunity to reduce oil and gas methane emissions in light of this study's results and global mitigation framework targets.

Algeria is the sixth largest gas-flaring country (World Bank GFMR, 2025), and despite a sustained flaring decline in the Illizi-Ghadames (-31%) and lower 2024 endpoint values in the Hassi R'Mel and Oued Mya (-13% and -14% from 2020 levels), flaring alone does not explain the emissions observed across Algeria. Particularly in oil-dominant areas, venting and fugitive emissions are likely significant—Naus et al. (2023) found that ten out of eleven superemitters were unlit flares, with these Sentinel-2-detectable sources (~3 t h^{-1} detection limit at Hassi Messaoud; Gorroño et al., 2023) accounting for 49 [27–71]% of total emissions in the oil-dominant Hassi Messaoud region but only 24 [12–40]% in the gas-dominant Hassi R'Mel. This dual significance of dispersed and point-source emissions has been observed across major producing regions globally (Williams et al., 2025; Warren et al., 2025) and reinforces that effective mitigation must address both source types. The possibly greater prevalence of high-emitting point sources in oil-dominant regions may partly explain the differences in emission totals observed across our study areas. Declining gas flaring counts may reflect flares being shut off rather than gas being captured, which would mean flaring reduction alone is insufficient. While superemitters represent an important mitigation opportunity, the spatial distribution of emissions observed in MethaneSAT data across all three regions suggests that dispersed area sources represent a significant contribution to total emissions, particularly in the oil-dominant Oued Mya. As such, the results of this analysis suggest that targeted mitigation in Oued Mya, including, for example, leak detection and repair (LDAR) programs, gas capture infrastructure to replace shuttered flares, and routine emissions monitoring, represents a high-leverage methane mitigation opportunity given its disproportionate contribution to Algeria's total emissions.

The Hassi R'Mel basin demonstrates that lower-emissions gas production is possible within Algeria, but the wide disparity between the other oil-dominant and mixed-oil and gas production regions underscores the need for fine-grained individual basin-level methane intensity tracking. This analysis is based on MethaneSAT data from its 13-month limited operational lifetime, which demonstrated the satellite's capabilities in characterizing regional emissions at high resolution, combining ~25–55 ppb precision at native pixel size of 110 m × 400 m with a wide regional mapping swath of ~220 km (Guanter et al., 2026). With the loss of MethaneSAT in June 2025, future basin-scale observations depend in part on the development and application of measurement strategies and capabilities with comparable spatial resolution and scope, in order to quantify basin- and sub-basin-scale emissions and monitor changes in methane intensity against mitigation targets over time.

Data availability

MethaneSAT Level 3 methane concentration maps and Level 4 area emissions data are publicly accessible through Google Earth Engine (https://developers.google.com/earth-engine/datasets/publisher/edf-methanesat-ee) and Google Cloud Storage (MethaneSAT, 2026). Field-level oil and gas production data were licensed from Wood Mackenzie and cannot be redistributed. VIIRS flaring volumes and the bottom-up inventories (GFEI v3, EDGAR, CAMS) are publicly available from their respective providers.

Supporting Information

Comparison of simple-subtraction and ratio-based sectoral disaggregation methods; sensitivity of gas-normalized methane intensity to methane composition assumptions; country-wide comparison with IEA estimates; IEA emission-factor analysis by region; U.S. basin comparison methodology and composition rescaling; Tables S1–S4

Acknowledgements

We thank the MethaneSAT mission operations team and the science and data processing teams for making the data products used in this study available.

Funding for MethaneSAT activities was provided in part by anonymous donors, Arnold Ventures, The Audacious Project, the Ballmer Group, the Bezos Earth Fund, The Children's Investment Fund Foundation, the Heising–Simons

Family Fund, King Philanthropies, the Robertson Foundation, the Skyline Foundation, and the Valhalla Foundation. For a more complete list of funders, please visit https://www.methanesat.org/ (last access: 1 April 2026).

Author contributions

Anthony Himmelberger: Conceptualization, Data Curation, Formal Analysis, Investigation, Methodology, Visualization, Writing – Original Draft, Writing – Review & Editing. Mark Omara: Conceptualization, Methodology, Project Administration, Supervision, Writing – Review & Editing. Marvin Knapp: Methodology, Software, Writing – Review & Editing. James P. Williams: Methodology, Software, Writing – Review & Editing. Kaiya Weatherby: Methodology, Writing – Review & Editing. Ben Lyke: Methodology, Writing – Review & Editing. Joshua Benmergui: Methodology, Software, Writing – Review & Editing. Katlyn MacKay: Methodology, Writing – Review & Editing. Jack Warren: Methodology, Writing – Review & Editing. Luis Guanter: Methodology, Writing – Review & Editing. Steven C. Wofsy: Methodology, Writing – Review & Editing. Ritesh Gautam: Conceptualization, Methodology, Project Administration, Supervision, Writing – Review & Editing.

References

Albriki, K., Wang, F., Li, M., El Zaroug, R., Ali, A., Samba, M., Wiping, F., and Mohammed, R. S.: Silurian hot shale occurrence and distribution, organofacies, thermal maturation, and petroleum generation in Ghadames Basin, North Africa, J. Afr. Earth Sci., 189, 104497, https://doi.org/10.1016/j.jafrearsci.2022.104497, 2022.

Alvarez, R. A., Zavala-Araiza, D., Lyon, D. R., Allen, D. T., Barkley, Z. R., Brandt, A. R., Davis, K. J., Herndon, S. C., Jacob, D. J., Karion, A., Kort, E. A., Lamb, B. K., Lauvaux, T., Maasakkers, J. D., Marchese, A. J., Omara, M., Pacala, S. W., Peischl, J., Robinson, A. L., Shepson, P. B., Sweeney, C., Townsend-Small, A., Wofsy, S. C., and Hamburg, S. P.: Assessment of methane emissions from the U.S. oil and gas supply chain, Science, 361, 186–188, https://doi.org/10.1126/science.aar7204, 2018.

Burdeau, P. M., Sherwin, E. D., Biraud, S. C., Berman, E. S. F., and Brandt, A. R.: High-resolution national mapping of natural gas composition substantially updates methane leakage impacts, Nat. Commun., 16, 11297, https://doi.org/10.1038/s41467-025-66465-6, 2025.

Carpenter, B., Gelman, A., Hoffman, M. D., Lee, D., Goodrich, B., Betancourt, M., Brubaker, M., Guo, J., Li, P., and Riddell, A.: Stan: a probabilistic programming language, J. Stat. Softw., 76, 1–32, https://doi.org/10.18637/jss.v076.i01, 2017.

Chen, Z., Jacob, D. J., Gautam, R., Omara, M., Stavins, R. N., Stowe, R. C., Nesser, H., Sulprizio, M. P., Lorente, A., Varon, D. J., Lu, X., Shen, L., Qu, Z., Pendergrass, D. C., and Hancock, S.: Satellite quantification of methane emissions and oil–gas methane intensities from individual countries in the Middle East and North Africa: implications for climate action, Atmos. Chem. Phys., 23, 5945–5967, https://doi.org/10.5194/acp-23-5945-2023, 2023.

Crippa, M., Guizzardi, D., Pagani, F., Schiavina, M., Melchiorri, M., Pisoni, E., Graziosi, F., Muntean, M., Maes, J., Dijkstra, L., Van Damme, M., Clarisse, L., and Coheur, P.: Insights into the spatial distribution of global, national, and subnational greenhouse gas emissions in the Emissions Database for Global Atmospheric Research (EDGAR v8.0), Earth System Science Data, 16, 2811–2830, https://doi.org/10.5194/essd-16-2811-2024, 2024.

East, J. D., Jacob, D. J., Jervis, D., Balasus, N., Estrada, L. A., Hancock, S. E., Sulprizio, M. P., Thomas, J., Wang, X., Chen, Z., Varon, D. J., and Worden, J. R.: Worldwide inference of national methane emissions by inversion of satellite observations with UNFCCC prior estimates, Nat. Commun., 16, 11004, https://doi.org/10.1038/s41467-025-67122-8, 2025.

European Parliament and Council of the European Union: Regulation (EU) 2024/1787 of the European Parliament and of the Council of 13 June 2024 on the reduction of methane emissions in the energy sector and amending Regulation (EU) 2019/942, Official Journal of the European Union, L 2024/1787, https://eur-lex.europa.eu/eli/reg/2024/1787/oj, last access: 17 March 2026, 2024.

Eurostat: Shedding light on energy in Europe — 2025 edition, European Commission, Luxembourg, https://ec.europa.eu/eurostat/web/interactive-publications/energy-2025, last access: 17 March 2026, 2025.

Fasoli, B., Lin, J. C., Bowling, D. R., Mitchell, L., and Mendoza, D.: Simulating atmospheric tracer concentrations for spatially distributed receptors: updates to the Stochastic Time-Inverted Lagrangian Transport model's R interface (STILT-R version 2), Geosci. Model Dev., 11, 2813–2824, https://doi.org/10.5194/gmd-11-2813-2018, 2018.

Galeazzi, S., Point, O., Haddadi, N., Mather, J., and Druesne, D.: Regional geology and petroleum systems of the Illizi-Berkine area of the Algerian Saharan Platform: an overview, Mar. Pet. Geol., 27, 143–178, https://doi.org/10.1016/j.marpetgeo.2009.07.007, 2010.

Global Energy Monitor: Global gas infrastructure tracker, Global Energy Monitor, November 2025 release, https://globalenergymonitor.org/projects/global-gas-infrastructure-tracker/, last access: 17 March 2026, 2025a.

Global Energy Monitor: Global oil and gas extraction tracker, Global Energy Monitor, February 2025 release, https://globalenergymonitor.org/projects/global-oil-gas-extraction-tracker/, last access: 17 March 2026, 2025b.

Global Methane Pledge (GMP): About the Global Methane Pledge, https://www.globalmethanepledge.org/, last access: 17 March 2026, 2026.

Gorroño, J., Varon, D. J., Irakulis-Loitxate, I., and Guanter, L.: Understanding the potential of Sentinel-2 for monitoring methane point emissions, Atmos. Meas. Tech., 16, 89–107, https://doi.org/10.5194/amt-16-89-2023, 2023.

Granier, C., Darras, S., Denier van Der Gon, H., Jana, D., Elguindi, N., Bo, G., Michael, G., Marc, G., Jalkanen, J.-P., Kuenen, J., Liousse, C., Quack, B., Simpson, D., and Sindelarova, K.: The Copernicus Atmosphere Monitoring Service global and regional emissions (April 2019 version), Copernicus Atmosphere Monitoring Service, https://doi.org/10.24380/d0bn-kx16, 2019.

Guanter, L., Roger, J., Warren, J., Sargent, M., Zhang, Z., Roche, S., Miller, C. C., Steiner, M., Hadfield, H., Omara, M., Williams, J., MacKay, K., Franklin, J. E., Luo, B., Wofsy, S. C., Hamburg, S. P., and Gautam, R.: Surveying methane point-source super-emissions across oil and gas basins with MethaneSAT, Atmospheric Chemistry and Physics, 26, 2941–2963, https://doi.org/10.5194/acp-26-2941-2026, 2026.

Hoffman, M. D. and Gelman, A.: The No-U-Turn Sampler: adaptively setting path lengths in Hamiltonian Monte Carlo, arXiv [preprint], https://doi.org/10.48550/arXiv.1111.4246, 18 November 2011.

International Energy Agency (IEA): Law No. 19-13 – law governing hydrocarbon activities, IEA Policies Database, https://www.iea.org/policies/11809-law-no-19-13-law-governing-hydrocarbon-activities, 2022, last access: 17 March 2026.

International Energy Agency (IEA): Global methane tracker 2024, IEA, Paris [Dataset], https://www.iea.org/reports/global-methane-tracker-2024, 2024, last access: 17 March 2026.

International Energy Agency (IEA): Global methane tracker 2025, IEA, Paris, https://www.iea.org/reports/global-methane-tracker-2025, 2025, last access: 17 March 2026.

International Monetary Fund (IMF): Algeria: 2023 Article IV consultation — staff report, IMF Country Report No. 2024/088, IMF, Washington, D.C., https://doi.org/10.5089/9798400271878.002, 2024.

IPCC: Climate change 2021: the physical science basis. Contribution of Working Group I to the Sixth Assessment Report of the Intergovernmental Panel on Climate Change, Cambridge University Press, Cambridge, https://doi.org/10.1017/9781009157896, 2021.

Jacob, D. J., Varon, D. J., Cusworth, D. H., Dennison, P. E., Frankenberg, C., Gautam, R., Guanter, L., Kelley, J., McKeever, J., Ott, L. E., Poulter, B., Qu, Z., Thorpe, A. K., Worden, J. R., and Duren, R. M.: Quantifying methane emissions from the global scale down to point sources using satellite observations of atmospheric methane, Atmos. Chem. Phys., 22, 9617–9646, https://doi.org/10.5194/acp-22-9617-2022, 2022.

Lan, X., Thoning, K. W., and Dlugokencky, E. J.: Trends in globally-averaged CH_4, N_2O, and SF_6 determined from NOAA Global Monitoring Laboratory measurements, Version 2026-03, NOAA Global Monitoring Laboratory, https://doi.org/10.15138/P8XG-AA10, 2025.

Lin, J. C., Gerbig, C., Wofsy, S. C., Andrews, A. E., Daube, B. C., Davis, K. J., and Grainger, C. A.: A near-field tool for simulating the upstream influence of atmospheric observations: the Stochastic Time-Inverted Lagrangian Transport (STILT) model, J. Geophys. Res., 108, 4493, https://doi.org/10.1029/2002JD003161, 2003.

MacKay, K., Benmergui, J., Williams, J. P., Omara, M., Himmelberger, A., Sargent, M., Warren, J. D., Miller, C. C., Roche, S., Zhang, Z., Franklin, J., Guanter, L., Wofsy, S., and Gautam, R.: Assessment of methane emissions from U.S. onshore oil and gas production using MethaneAIR measurements, Atmos. Chem. Phys., 26, 1179–1192, https://doi.org/10.5194/acp-26-1179-2026, 2026.

MethaneSAT: MethaneSAT loses contact with satellite, Environmental Defense Fund, https://www.methanesat.org/project-updates/methanesat-loses-contact-satellite, last access: 17 March 2026, 2025.

MethaneSAT: MethaneSAT Level-3 and Level-4 methane data products, Environmental Defense Fund / Google Earth Engine [Data set], https://developers.google.com/earth-engine/datasets/publisher/edf-methanesat-ee, last access: 17 March 2026, 2026.

MethaneSAT Science and Engineering Team: MethaneSAT Level-4 dispersed emissions product: algorithm theoretical basis document v1.1, Zenodo, https://doi.org/10.5281/zenodo.19873046, 2026.

Naus, S., Maasakkers, J. D., Gautam, R., Omara, M., Stikker, R., Veenstra, A. K., Nathan, B., Irakulis-Loitxate, I., Guanter, L., Pandey, S., Girard, M., Lorente, A., Borsdorff, T., and Aben, I.: Assessing the relative importance of satellite-detected methane superemitters in quantifying total emissions for oil and gas production areas in Algeria, Environ. Sci. Technol., 57, 19545–19556, https://doi.org/10.1021/acs.est.3c04746, 2023.

Ocko, I. B., Sun, T., Shindell, D., Oppenheimer, M., Hristov, A. N., Pacala, S. W., Mauzerall, D. L., Xu, Y., and Hamburg, S. P.: Acting rapidly to deploy readily available methane mitigation measures by sector can immediately slow global warming, Environ. Res. Lett., 16, 054042, https://doi.org/10.1088/1748-9326/abf9c8, 2021.

Oil and Gas Climate Initiative (OGCI): 2024 progress report, OGCI, London, https://www.ogci.com/our-progress/progress-reports/, last access: 17 March 2026, 2024.

Oil and Gas Decarbonization Charter (OGDC): About the charter, https://www.ogdc.org/about/, last access: 17 March 2026, 2025.

Omara, M., Gautam, R., O'Brien, M. A., Himmelberger, A., Franco, A., Meisenhelder, K., Hauser, G., Lyon, D. R., Chulakadabba, A., Miller, C. C., Franklin, J., Wofsy, S. C., and Hamburg, S. P.: Developing a spatially explicit global oil and gas infrastructure database for characterizing methane emission sources at high resolution, Earth Syst. Sci. Data, 15, 3761–3790, https://doi.org/10.5194/essd-15-3761-2023, 2023.

Scarpelli, T. R., Roy, E., Jacob, D. J., Sulprizio, M. P., Tate, R. D., and Cusworth, D. H.: Using new geospatial data and 2020 fossil fuel methane emissions for the Global Fuel Exploitation Inventory (GFEI) v3, Earth Syst. Sci. Data, 17, 7019–7033, https://doi.org/10.5194/essd-17-7019-2025, 2025.

Seymour, S., Xie, D., Kang, M., Schwietzke, S., Zavala-Araiza, D., Hamburg, S.P. Methane emission intensity metrics: unmasking the trade-offs. [Preprint], https://doi.org/10.21203/rs.3.rs-6753363/v1, 2025.

Shen, L., Jacob, D. J., Gautam, R., Omara, M., Scarpelli, T. R., Lorente, A., Zavala-Araiza, D., Lu, X., Chen, Z., and Lin, J.: National quantifications of methane emissions from fuel exploitation using high resolution inversions of satellite observations, Nat. Commun., 14, 4948, https://doi.org/10.1038/s41467-023-40671-6, 2023.

Tahchi, B.: Algerian gas to strengthen energy security of the European Union: policy, capacity and strategy, Energy Rep., 11, 1511–1528, https://doi.org/10.1016/j.egyr.2024.01.009, 2024.

Talus, K., Steck, G., and Atkin, J.: EU methane regulation and its impact on LNG imports, J. World Energy Law Bus., 18, jwae022, https://doi.org/10.1093/jwelb/jwae022, 2024.

Tibrewal, K., Ciais, P., Saunois, M., Martinez, A., Lin, X., Thanwerdas, J., Deng, Z., Chevallier, F., Giron, C., and Albergel, C.: Assessment of methane emissions from oil, gas and coal sectors across inventories and atmospheric inversions, Commun. Earth Environ., 5, 26, https://doi.org/10.1038/s43247-023-01190-w, 2024.

United Nations Economic Commission for Europe (UNECE): The EU methane regulation: global implications, benefits and challenges, UNECE, Geneva, https://unece.org/sustainable-energy/events/eu-methane-regulation-global-implications-benefits-and-challenges, last access: 17 March 2026, 2025.

United Nations Environment Programme (UNEP): An eye on methane — invisible but not unseen: how data-driven tools can turn the tide on methane emissions — if we use them, UNEP, Nairobi, https://www.unep.org/resources/eye-methane-2024, last access: 17 March 2026, 2024.

U.S. Energy Information Administration (EIA): Country analysis brief: Algeria, EIA, Washington, D.C., https://www.eia.gov/international/content/analysis/countries_long/Algeria/algeria.PDF, last access: 17 March 2026, 2025.

U.S. Environmental Protection Agency (EPA): Biden-Harris administration finalizes standards to slash methane pollution, combat climate change, protect health, and bolster American innovation, https://www.epa.gov/newsreleases/biden-harris-administration-finalizes-standards-slash-methane-pollution-combat-climate, last access: 17 March 2026, 2023.

UK Department for Energy Security and Net Zero (DESNZ): Diversity of supply of natural gas in Europe 2024, Energy Trends special article, HM Government, London, https://assets.publishing.service.gov.uk/media/69403a5f33c7ace9c4a42207/Diversity_of_supply_of_natural_gas_in_Europe_2024.pdf, last access: 17 March 2026, 2025.

Warren, J. D., Sargent, M., Williams, J. P., Omara, M., Miller, C. C., Roche, S., MacKay, K., Manninen, E., Chulakadabba, A., Himmelberger, A., Benmergui, J., Zhang, Z., Guanter, L., Wofsy, S., and Gautam, R.: Sectoral contributions of high-emitting methane point sources from major US onshore oil and gas producing basins using airborne measurements from MethaneAIR, Atmos. Chem. Phys., 25, 10661–10675, https://doi.org/10.5194/acp-25-10661-2025, 2025.

Williams, J. P., Omara, M., Himmelberger, A., Zavala-Araiza, D., MacKay, K., Benmergui, J., Sargent, M., Wofsy, S. C., Hamburg, S. P., and Gautam, R.: Small emission sources in aggregate disproportionately account for a large majority of total methane emissions from the US oil and gas sector, Atmos. Chem. Phys., 25, 1513–1532, https://doi.org/10.5194/acp-25-1513-2025, 2025.

Williams, J. P., Benmergui, J., Knapp, M., Omara, M., Himmelberger, A., Kyzivat, E., Weatherby, K., Lyke, B., Warren, J., MacKay, K., Ayvazov, S., Russi, M., LoFaso, N., Melendez, T., Miller, C. C., Roche, S., Sargent, M., Franklin, J., Nasr, M., Zhang, Z., Miller, D. J., Luo, B., Guanter, L., Hamburg, S. P., Wofsy, S. C., and Gautam, R.: Methane intensity and emissions across major oil and gas basins and individual jurisdictions using MethaneSAT observations, Atmos. Chem. Phys., 26, 5961–5981, https://doi.org/10.5194/acp-26-5961-2026, 2026.

Wood Mackenzie: Wood Mackenzie Lens, Wood Mackenzie Ltd. [Data set], Edinburgh, https://www.woodmac.com/lens/, last access: 15 November 2025, 2024.

Worden, J. R., Cusworth, D. H., Qu, Z., Yin, Y., Zhang, Y., Bloom, A. A., Ma, S., Byrne, B. K., Scarpelli, T., Maasakkers, J. D., Crisp, D., Duren, R., and Jacob, D. J.: The 2019 methane budget and uncertainties at 1° resolution and each country through Bayesian integration of GOSAT total column methane data and a priori inventory estimates, Atmos. Chem. Phys., 22, 6811–6841, https://doi.org/10.5194/acp-22-6811-2022, 2022.

World Bank Global Flaring and Methane Reduction Partnership (GFMR): Global gas flaring tracker report, June 2024, World Bank [Data set], Washington, D.C., https://thedocs.worldbank.org/en/doc/d01b4aebd8a10513c0e341de5e1f652e-0400072024/original/Global-Gas-Flaring-Tracker-Report-June-20-2024.pdf, last access: 17 March 2026, 2024.

World Bank Global Flaring and Methane Reduction Partnership (GFMR): Global gas flaring tracker report, July 2025, World Bank [Data set], Washington, D.C., https://www.worldbank.org/en/programs/gasflaringreduction/publication/2025-global-gas-flaring-tracker-report, last access: 17 March 2026, 2025.

For Table of Contents Only

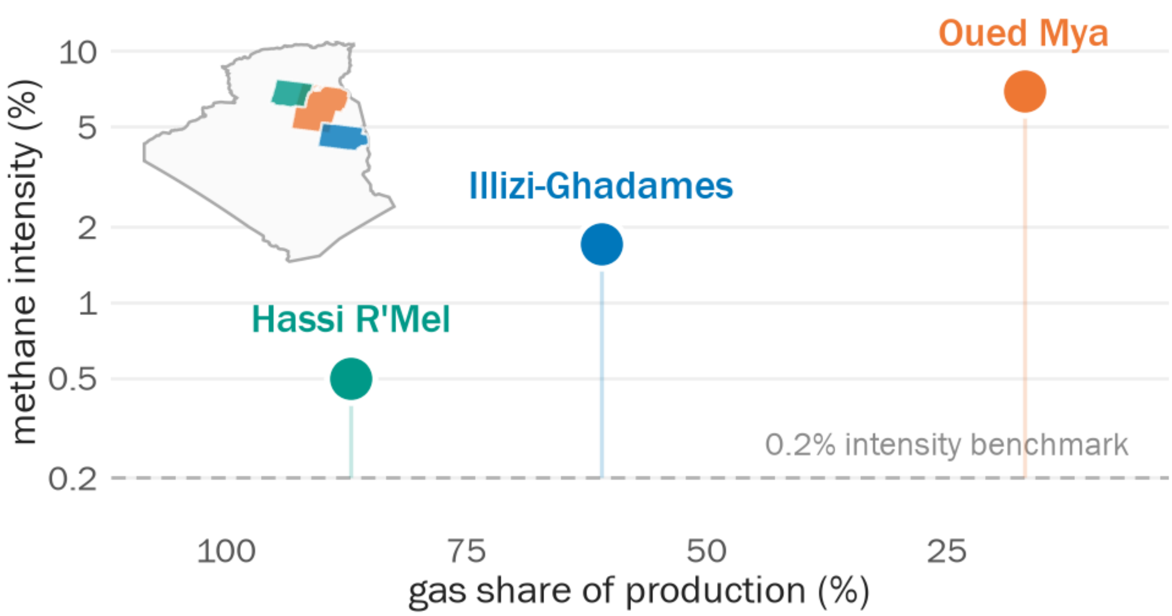

Supplement for

Contrasting oil and gas methane emission intensities across Algeria's major production basins derived using MethaneSAT data

Anthony Himmelberger*[1,^], Mark Omara*[2], Marvin Knapp[2,3], James P. Williams[2], Kaiya Weatherby[2], Ben Lyke[2], Joshua Benmergui[2,3], Katlyn MacKay[2], Jack Warren[2], Luis Guanter[2,4], Steven C. Wofsy[3], Ritesh Gautam[2]

[1] MethaneSAT, LLC, Austin, TX, USA 78701
[2] Environmental Defense Fund, New York, NY, USA 10010
[3] Harvard University, Cambridge, MA, USA 02138
[4] Research Institute of Water and Environmental Engineering (IIAMA), Universitat Politècnica de València, Valencia, Spain

Correspondence to: Anthony Himmelberger (anthony.himmelberger@maine.edu), Mark Omara (momara@edf.org)
^Present address: University of Maine, Orono, ME, USA 04401

S1. Sectoral disaggregation: comparison of simple subtraction and ratio-based methods

We allocate total MethaneSAT methane emissions to the oil and gas sector using a simple subtraction (SS) of a literature-based non-oil and gas estimate from the total domain emissions. This methodology was also used by MacKay et al. (2026). We tested a composite prior-based ratio method (RB) following the approach described in Williams et al. (2026), which uses a stacked prior inventory of spatially explicit bottom-up datasets to estimate the proportion of total emissions attributable to the oil and gas sector. The datasets used are GFEI v3 (Scarpelli et al., 2025), EDGAR v2025 (Crippa et al., 2024), CAMS v6.2 (Granier et al., 2019), and Carbon Mapper point-source observations (Carbon Mapper, 2026), and WetCHARTs v1.3.1 (Bloom et al., 2021). Table S1 compares oil and gas emission estimates and 95% confidence intervals from both methods across the three study regions.

The RB method attributes higher proportions of total emissions to non-oil and gas sources in all three regions, most starkly in the Hassi R'Mel, where 38% of total emissions would be attributed to non-oil and gas sources. The SS method attributes ~10% of Hassi R'Mel emissions to non-oil and gas sources, a more reasonable estimate given the concentration of oil and gas activity in the Hassi R'Mel field and non-significant contribution non-oil and gas sources based on prior literature (East et al., 2025). The same directional pattern holds in the Oued Mya (RB: 17% non-OG vs. SS: 7.0%) and, in the Illizi-Ghadames (RB: 9% vs. SS: 1.2%). We therefore adopt the simple subtraction method as the primary approach for this study.

Table S1. Comparison of oil and gas methane emission estimates ($t\ h^{-1}$) from the Simple Subtraction (SS) and Ratio-Based (RB) sectoral disaggregation methods for each study region. Upper and lower bounds represent 95% confidence intervals combining aggregation and sectoral disaggregation uncertainty. Non-OG % indicates the proportion of total MethaneSAT domain emissions attributed to non-oil and gas sources under each method.

Region	Method	Total Emissions ($t\ h^{-1}$)	OG Mean ($t\ h^{-1}$)	OG Upper ($t\ h^{-1}$)	OG Lower ($t\ h^{-1}$)	Non-OG %
Hassi R'Mel	RB	18	11	17	6	38%
Hassi R'Mel	SS	18	16	24	9	10%
Illizi-Ghadames	RB	25	23	36	12	9%

Illizi-Ghadames	SS	25	25	39	13	1.2%
Oued Mya	RB	48	39	56	23	17%
Oued Mya	SS	48	44	63	26	7.0%

S2. Sensitivity of gas-normalized methane intensity to methane composition

Gas-normalized methane intensity (loss rate) is calculated as oil and gas methane emissions divided by marketed gas production adjusted for methane composition. This study uses a uniform methane composition of 0.90 for all three regions, consistent with pipeline-quality gas specifications (Alvarez et al., 2018; Shen et al., 2023). To assess the sensitivity of our results to this assumption, we recalculate loss rates using a range of alternative composition values drawn from spatially explicit estimates for structurally similar U.S. basins (Burdeau et al., 2025): the Haynesville basin (0.98; dry gas, comparable to Hassi R'Mel), the Eagle Ford basin (0.79; mixed production, comparable to Illizi-Ghadames), and the Permian basin (0.72; oil-dominant, comparable to Oued Mya). We also include the composition assumed in Williams et al. (2026) of 0.80 for reference. Energy-normalized methane intensity (kg CH_4 GJ^{-1}) does not incorporate a methane composition assumption and is therefore unaffected by this sensitivity test.

Table S2 presents loss rates for each region under each composition assumption. Across all tested values, the relative ordering of the three regions is preserved: Hassi R'Mel consistently shows the lowest intensity, Oued Mya the highest, and Illizi-Ghadames intermediate. The absolute effect of the methane composition assumption is largest in Oued Mya, where the range spans 6.4% (at 0.98) to 8.7% (at 0.72), and smallest in Hassi R'Mel, where the range spans 0.42% to 0.58%. The paper's 0.90 assumption produces results near the middle of this range for all three regions.

Table S2. Sensitivity of gas-normalized methane intensity (%) to methane composition assumption for each study region. Emissions and gas production values are from the primary analysis (area-adjusted)((Wood Mackenzie, 2024). The composition assumed in the main text (0.90) is bolded. Energy-normalized intensity (kg CH_4 GJ^{-1}) is unaffected by composition and is not shown here.

Region	0.98 (Haynesville)	0.90 (this study)	0.80 (Williams et al.)	0.79 (Eagle Ford)	0.72 (Permian)
Hassi R'Mel	0.42%	**0.46%**	0.52%	0.52%	0.58%
Illizi-Ghadames	1.6%	**1.7%**	1.9%	1.9%	2.1%
Oued Mya	6.4%	**6.9%**	7.9%	8.0%	8.7%

S3. IEA country-wide comparison

A country-wide comparison with IEA 2024 estimates shows total oil and gas methane emissions of 317.5 t h^{-1} for all of Algeria (IEA, 2024), compared to this study's three-region oil and gas total of 80 t h^{-1} [50–111 t h^{-1}], which covers 73% of Algeria's total onshore oil and gas production. Our combined methane intensity of 1.5% [0.94–2.1%] is lower than IEA's country-wide estimate of 4.3%.

At a 2024 average TTF price of USD 11 $MMBtu^{-1}$ (IEA, 2025), the combined three-region emissions represent approximately USD 401 M yr^{-1} or €369 M yr^{-1} in lost gas value. Region-level breakdown: Hassi R'Mel ~USD 79 M yr^{-1}, Illizi-Ghadames ~USD 125 M yr^{-1}, Oued Mya ~USD 222 M yr^{-1}. This calculation converts annual totals using t h^{-1} × 8,760 h yr^{-1} and 52.07 MMBtu t^{-1} (gross calorific value basis) and represents a theoretical upper bound assuming full capture and sale at market price.

Note that the IEA country-wide estimate encompasses all of Algeria's onshore and offshore production and employs different methodological assumptions than the MethaneSAT region-level analysis presented in the main text. Direct comparison between the two should therefore be interpreted cautiously. The three-region MethaneSAT total covers 73% of Algeria's onshore oil and gas production; the remaining 27% of production, and any offshore emissions, are not captured in our estimate.

S4. IEA emissions factor analysis by region

To further contextualize MethaneSAT observations against IEA country-wide estimates, we derive IEA-implied emission factors from the country-wide Algeria total (317.5 t h^{-1}; IEA, 2024) normalized by WoodMac 2024 production data, and apply these factors to each study region. Three normalizations are presented: gas-production-normalized, oil-production-normalized, and total-production-normalized emission factors.

IEA country-wide emission factors: 187.1 kg h^{-1} per kboe d^{-1} (gas-normalized), 237.4 kg h^{-1} per kboe d^{-1} (oil-normalized), and 104.6 kg h^{-1} per kboe d^{-1} (total-production-normalized).

Table S3. IEA-implied versus MethaneSAT-observed methane emissions by region, using a total-production-normalized IEA emission factor (104.6 kg h^{-1} per kboe d^{-1}). MSAT/IEA ratio < 1 indicates MethaneSAT observes lower emissions than IEA implies; ratio > 1 indicates higher. Note that the combined total emissions is lower than the sum of emissions in individual regions because of the overlap in observation domains (see Figure 1 in Main Text)

Region	Production (kboe d^{-1})	IEA-implied (t h^{-1})	MethaneSAT observed O&G (t h^{-1})	MSAT/IEA ratio
Hassi R'Mel	912	95	16	0.17
Oued Mya	842	88	44	0.50
Illizi-Ghadames	558	58	25	0.43
Combined	**2,203**	**231**	**80**	**0.35**

The gas- and oil-normalized ratios show strong regional differentiation. Gas-normalized: Hassi R'Mel 0.11, Oued Mya 1.62, Illizi-Ghadames 0.39. Oil-normalized: Hassi R'Mel 0.57, Oued Mya 0.27, Illizi-Ghadames 0.48. These ratios reflect the mismatch between IEA's country-level emission factor — which implicitly assumes a uniform emissions profile across Algeria — and the wide regional variability observed by MethaneSAT. The Hassi R'Mel gas-normalized ratio of 0.11 is consistent with its low-intensity performance relative to IEA expectations; the Oued Mya gas-normalized ratio of 1.62 reflects the structural inflation of gas-normalized metrics in oil-dominant regions discussed in the main text.

S5. U.S. basin comparison: methodology and composition rescaling

To contextualize Algeria's methane intensities against well-characterized U.S. basins measured by MethaneAIR (MacKay et al., 2026) and MethaneSAT (Williams et al., 2026), we pair each Algerian region with a structurally similar U.S. basin based on production type: Hassi R'Mel (87% gas) with the Haynesville-Bossier basin (99% gas; MacKay et al., 2026), Illizi-Ghadames (61% gas) with the Eagle Ford basin (47–53% gas; MacKay et al., 2026; Williams et al., 2026), and Oued Mya (83% oil) with the Permian basin (~60% oil; MacKay et al., 2026; Williams et al., 2026). Because U.S. studies assume different methane compositions (0.73–0.86 in MacKay et al., 2026; 0.80 in Williams et al., 2026) compared to this study (0.90), we rescale U.S. gas-normalized intensities to a common composition of 0.90 for direct comparison using:

Adjusted intensity = Reported intensity × (Reported composition / 0.90)

Energy-normalized intensities (kg CH_4 GJ^{-1}) do not incorporate a methane composition assumption and are therefore directly comparable across studies without rescaling. Table S4 presents the adjusted and unadjusted intensities for each U.S. basin alongside the corresponding Algerian region.

Table S4. Comparison of gas-normalized and energy-normalized methane intensities between Algerian study regions and structurally similar U.S. basins. U.S. gas-normalized intensities are adjusted to a common methane composition of 0.90 for direct comparison. Energy-normalized intensities are directly comparable without adjustment. U.S. values from MacKay et al. (2026) and Williams et al. (2026).

Algerian Region	U.S. Analog	Production Type	Algeria Gas-Norm. (%)	U.S. Gas-Norm. Adjusted to 0.90 (%)	Algeria Energy-Norm. (kg CH_4 GJ^{-1})	U.S. Energy-Norm. (kg CH_4 GJ^{-1})
Hassi R'Mel	Haynesville-Bossier	Gas-dominant	0.46%	0.86%	0.07	0.15
Illizi-Ghadames	Eagle Ford	Mixed	1.7%	1.6–2.1%	0.19	0.13–0.21
Oued Mya	Permian	Oil-dominant	6.9%	2.1–2.3%	0.22	0.15–0.16

References

Alvarez, R. A., Zavala-Araiza, D., Lyon, D. R., Allen, D. T., Barkley, Z. R., Brandt, A. R., Davis, K. J., Herndon, S. C., Jacob, D. J., Karion, A., Kort, E. A., Lamb, B. K., Lauvaux, T., Maasakkers, J. D., Marchese, A. J., Omara, M., Pacala, S. W., Peischl, J., Robinson, A. L., Shepson, P. B., Sweeney, C., Townsend-Small, A., Wofsy, S. C., and Hamburg, S. P.: Assessment of methane emissions from the U.S. oil and gas supply chain, Science, 361, 186–188, https://doi.org/10.1126/science.aar7204, 2018.

Bloom, A. A., Bowman, K. W., Lee, M., Turner, A. J., Schroeder, R., Worden, J. R., Weidner, R. J., McDonald, K. C., and Jacob, D. J.: CMS: Global 0.5-deg wetland methane emissions and uncertainty (WetCHARTs v1.3.1), ORNL DAAC, Oak Ridge, Tennessee, USA [data set], https://doi.org/10.3334/ORNLDAAC/1915, 2021.

Burdeau, P. M., Sherwin, E. D., Biraud, S. C., Berman, E. S. F., and Brandt, A. R.: High-resolution national mapping of natural gas composition substantially updates methane leakage impacts, Nat. Commun., 16, 11297, https://doi.org/10.1038/s41467-025-66465-6, 2025.

Carbon Mapper: Carbon Mapper data portal, Carbon Mapper, Inc. [data set], https://data.carbonmapper.org, last access: 29 April 2026.

Crippa, M., Guizzardi, D., Pagani, F., Schiavina, M., Melchiorri, M., Pisoni, E., Graziosi, F., Muntean, M., Maes, J., Dijkstra, L., Van Damme, M., Clarisse, L., and Coheur, P.: Insights into the spatial distribution of global, national, and subnational greenhouse gas emissions in the Emissions Database for Global Atmospheric Research (EDGAR v8.0), Earth Syst. Sci. Data, 16, 2811–2830, https://doi.org/10.5194/essd-16-2811-2024, 2024.

Granier, C., Darras, S., Denier van Der Gon, H., Jana, D., Elguindi, N., Bo, G., Michael, G., Marc, G., Jalkanen, J.-P., Kuenen, J., Liousse, C., Quack, B., Simpson, D., and Sindelarova, K.: The Copernicus Atmosphere Monitoring Service global and regional emissions (April 2019 version), Copernicus Atmosphere Monitoring Service, https://doi.org/10.24380/d0bn-kx16, 2019.

International Energy Agency (IEA): Global methane tracker 2024, IEA, Paris [data set], https://www.iea.org/reports/global-methane-tracker-2024 (last access: 17 March 2026), 2024.

International Energy Agency (IEA): Gas market report, Q1-2025, IEA, Paris, https://iea.blob.core.windows.net/assets/6bd6c46d-21d7-4ae7-af9f-25dc9f8e7f3b/GasMarketReport,Q1-2025.pdf, 2025, last access: 17 March 2026.

MacKay, K., Benmergui, J., Williams, J. P., Omara, M., Himmelberger, A., Sargent, M., Warren, J. D., Miller, C. C., Roche, S., Zhang, Z., Franklin, J., Guanter, L., Wofsy, S., and Gautam, R.: Assessment of methane emissions from U.S. onshore oil and gas production using MethaneAIR measurements, Atmos. Chem. Phys., 26, 1179–1192, https://doi.org/10.5194/acp-26-1179-2026, 2026.

Scarpelli, T. R., Roy, E., Jacob, D. J., Sulprizio, M. P., Tate, R. D., and Cusworth, D. H.: Using new geospatial data and 2020 fossil fuel methane emissions for the Global Fuel Exploitation Inventory (GFEI) v3, Earth Syst. Sci. Data, 17, 7019–7033, https://doi.org/10.5194/essd-17-7019-2025, 2025.

Shen, L., Jacob, D. J., Gautam, R., Omara, M., Scarpelli, T. R., Lorente, A., Zavala-Araiza, D., Lu, X., Chen, Z., and Lin, J.: National quantifications of methane emissions from fuel exploitation using high resolution inversions of satellite observations, Nat. Commun., 14, 4948, https://doi.org/10.1038/s41467-023-40671-6, 2023.

Williams, J. P., Benmergui, J., Knapp, M., Omara, M., Himmelberger, A., Kyzivat, E., Weatherby, K., Lyke, B., Warren, J., MacKay, K., Ayvazov, S., Russi, M., LoFaso, N., Melendez, T., Miller, C. C., Roche, S., Sargent, M., Franklin, J., Nasr, M., Zhang, Z., Miller, D. J., Luo, B., Guanter, L., Hamburg, S. P., Wofsy, S. C., and Gautam, R.: Methane intensity and emissions across major oil and gas basins and individual jurisdictions using MethaneSAT observations, Atmos. Chem. Phys., 26, 5961–5981, https://doi.org/10.5194/acp-26-5961-2026, 2026.

Wood Mackenzie: Wood Mackenzie Lens, Wood Mackenzie Ltd. [data set], Edinburgh, https://www.woodmac.com/lens/, last access: 15 November 2025, 2024.